

# Compact Single-Chip *W*-Band FMCW Radar Modules for Commercial High-Resolution Sensor Applications

Axel Tessmann, Steffen Kudszus, *Member, IEEE*, Tobias Feltgen, Markus Riessle, Christoph Sklarczyk, and William H. Haydl

**Abstract**—Two compact single-chip 94-GHz frequency-modulated continuous-wave (FMCW) radar modules have been developed for high-resolution sensing under adverse conditions and environments. The first module contains a monolithic microwave integrated circuit (MMIC) consisting of a mechanically and electrically tunable voltage-controlled oscillator (VCO) with a buffer amplifier, 10-dB coupler, medium-power and a low-noise amplifier, balanced rat-race high electron-mobility transistor (HEMT) diode mixer, and a driver amplifier to increase the local-oscillator signal level. The overall chip-size of the FMCW radar MMIC is  $2 \times 3.5 \text{ mm}^2$ . For use with a single transmit-receive antenna, a 94-GHz microstrip hexaferite circulator was implemented in the module. The radar sensor achieved a tuning range of 1 GHz, an output signal power of 1.5 mW, and a conversion loss of 2 dB. The second FMCW radar sensor uses an MMIC consisting of a varactor-tuned VCO with injection port, very compact transmit and receive amplifiers, and a single-ended resistive mixer. To enable single-antenna operation, the external circulator was replaced by a combination of a Wilkinson divider and a Lange coupler integrated on the MMIC. The circuit features coplanar technology and cascode HEMTs for compact size and low cost. These techniques result in a particularly small overall chip-size of only  $2 \times 3 \text{ mm}^2$ . The packaged 94-GHz FMCW radar module achieved a tuning range of 6 GHz, an output signal power of 1 mW, and a conversion loss of 5 dB. The RF performance of the radar module was successfully verified by real-time monitoring the time flow of a gas-assisted injection molding process.

**Index Terms**—Coplanar waveguides (CPWs), flip-chip, frequency-modulated continuous-wave (FMCW) radar, GaAs, monolithic microwave integrated circuits (MMICs), packaging, *W*-band.

## I. INTRODUCTION

**I**N ADDITION to the forward-looking automotive radar, compact and efficient industrial sensors are the most promising commercial applications at *W*-band frequencies. They are suitable to control industrial manufacturing processes by contactless real-time monitoring the fabrication flow. Further applications are surface analysis, characterization of thin films on coated windows, quality control of welded joints, and level sensing. In

Manuscript received April 5, 2002; revised August 23, 2002.

A. Tessmann, T. Feltgen, M. Riessle, and W. H. Haydl are with the Fraunhofer Institute for Applied Solid State Physics, D-79108 Freiburg, Germany (e-mail: tessmann@iaf.fhg.de).

S. Kudszus was with the Fraunhofer Institute for Applied Solid State Physics, D-79108 Freiburg, Germany. He is now with Big Bear Networks, Milpitas, CA 95035 USA.

C. Sklarczyk is with the Fraunhofer Institute for Non-Destructive Testing, D-66123 Saarbruecken, Germany.

Digital Object Identifier 10.1109/TMTT.2002.805162

contrast to ultrasonic, video, infrared, and laser sensors, radar sensors are less sensitive to environmental conditions so they can be used to penetrate vapor, heat, and dust. Signal frequencies at *W*-band are very attractive due to their high spatial resolution, the resulting compact chip size, and small antenna dimensions [1]–[4]. For short-distance sensing, the signal output power is small, which is advantageous in many applications to reduce heating of both the test object and the sensor itself.

In this paper, we present two low-cost single-chip 94-GHz frequency-modulated continuous-wave (FMCW) radar modules. The monolithically integrated coplanar radar circuits include all components required for FMCW operation. The coplanar waveguide (CPW) technology is very attractive at millimeter-wave frequencies due to the simplified fabrication process and its potential for flip-chip packaging [5]. The cascode devices used in the amplifiers offer twice the gain of conventional high electron-mobility transistors (HEMTs) in a common-source configuration, while requiring the same chip area. For manufacturing the radar chips, we used a pseudomorphic AlGaAs/InGaAs/GaAs HEMT technology with molecular beam epitaxy (MBE) growth on semi-insulating 4-in wafers. The T-shaped  $0.15\text{-}\mu\text{m}$  gates were written with e-beam, and the recess was dry etched. The transistors typically achieve a transit frequency  $f_t = 100 \text{ GHz}$  and a maximum oscillation frequency  $f_{\max} = 180 \text{ GHz}$ . With 25% indium in the channel, a current density  $I_{\text{sat}}$  of 1000 mA/mm is achieved. The extrinsic maximum transconductance is 800 mS/mm. The *W*-band FMCW radar monolithic microwave integrated circuits (MMICs) were packaged in WR-10 waveguide modules, using CPW-to-waveguide transitions, realized on  $127\text{-}\mu\text{m}$ -thick quartz substrates. In addition to the conventional face-up mounting technique, we also investigated flip-chip packaging of the radar MMICs on doped silicon (n-Si) carriers [6].

The monolithically integrated multifunctional radar chips, low fabrication cost, small module size, and low weight combined with improved assembly techniques allow for the realization of high-performance *W*-band sensors highly suitable for commercial applications and industrial markets.

## II. 94-GHz FMCW RADAR MODULE #1 WITH HYBRID HEXAFERRITE CIRCULATOR ASSEMBLY

### A. Circuit Design and Packaging

A block diagram of the FMCW radar module #1 is shown in Fig. 1. The sensor incorporates a transceiver MMIC, a hexafer-

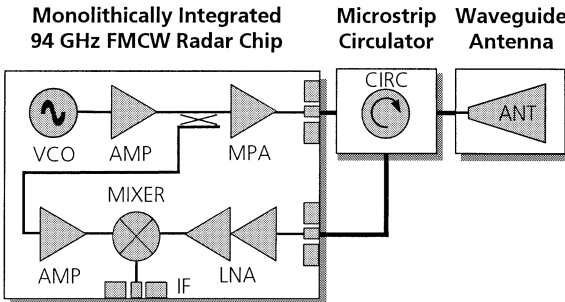


Fig. 1. Block diagram of the 94-GHz FMCW radar module #1 consisting of a GaAs MMIC, hexaferite circulator, and waveguide antenna.

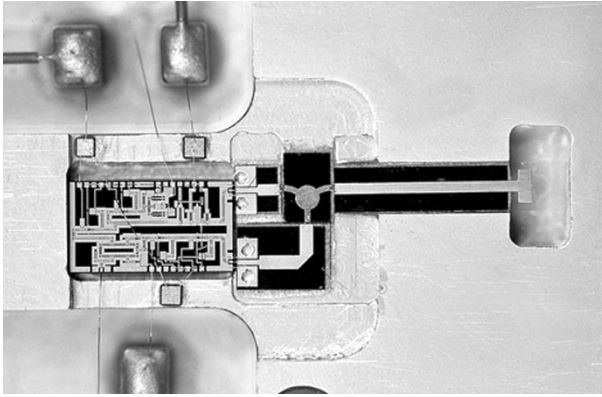


Fig. 2. Inside view of the 94-GHz FMCW radar module #1 with hybrid hexaferite circulator assembly.

rite microstrip circulator, CPW-to-microstrip transitions, and a waveguide antenna. The key component is the integrated transceiver MMIC, incorporating all components for FMCW radar operation: A voltage-controlled oscillator (VCO) with buffer amplifier (AMP) as the signal source, a 10-dB line coupler, and a medium power amplifier (MPA) in the transmit path. The receive path is formed by a low-noise amplifier (LNA), a balanced rat-race HEMT diode mixer (MIXER), and a driver amplifier to increase the local oscillator (LO) signal level. The oscillator is electrically tunable with the gate voltage of the VCO HEMT. Additionally mechanical adjustment of the center frequency is possible by removing air bridges in the source lines [7]. A cascode buffer amplifier raises the output power and improves the isolation of the oscillator. A fraction of the transmit signal is coupled out, amplified, and used as the LO signal for the mixer. A two-stage common source MPA feeds the circulator with the transmit power. In the receive path, a single balanced rat-race hybrid mixer is utilized to generate the IF from the LO signal and the received signal, which is amplified by a two-stage cascode LNA [8]. The chip size of the FMCW radar MMIC is  $2 \times 3.5 \text{ mm}^2$ .

As shown in Fig. 2, all components were mounted in a gold-plated steel package, utilizing conductive epoxy, except for the circulator, which had to be attached with nonconductive epoxy to ensure a proper functionality. The hexaferite microstrip circulator is a product of the Dorado International Corporation, Seattle, WA, and requires no external magnetic biasing [9]. Coplanar-to-microstrip transitions have been realized on  $127\text{-}\mu\text{m}$ -thick quartz substrates using a pair of ground-via

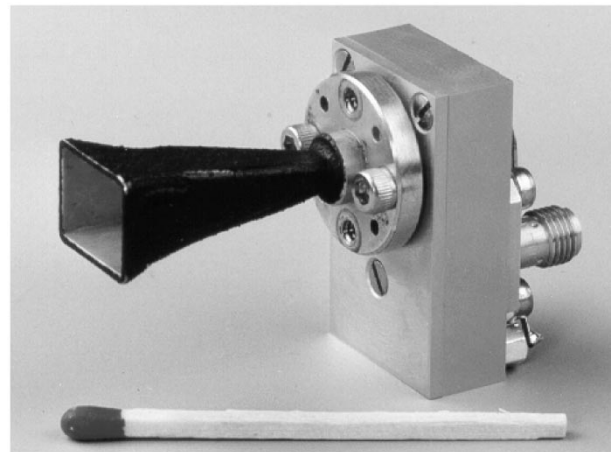


Fig. 3. Photograph of the 94-GHz FMCW radar module #1 with microstrip hexaferite circulator.

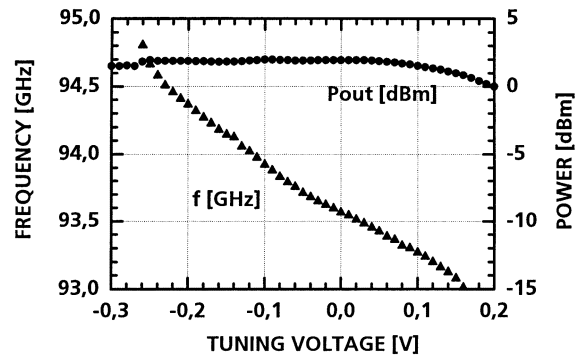


Fig. 4. Radar module #1. Measured output power and signal frequency as a function of the tuning voltage.

connections. To be compatible with standard waveguide horn antennas, a microstrip-to-waveguide transition has been developed using the Agilent HFSS simulator for optimization (see Section III). The transition is based on a conventional *E*-plane probe and placed into a WR-10 waveguide with back short. The width of the quartz substrate was chosen to eliminate possible waveguide modes in the microstrip cavity. The bond-wire interconnections were as short as possible using wedge-bonded  $17\text{-}\mu\text{m}$  gold wires. Chip capacitors of  $120 \text{ pF}$ , surface-mounted device (SMD) ceramic capacitors of  $10 \text{ nF}$ , and bias filters have been implemented in the module to prevent low-frequency oscillations. We used SMA connectors for the IF and FM port, resulting in a package size of only  $33 \times 20 \times 9.5 \text{ mm}^3$ . A photograph of the 94-GHz FMCW radar module is shown in Fig. 3.

### B. Performance and Experimental Results

The measured output power and signal frequency of the integrated VCO are shown in Fig. 4 as a function of the tuning voltage. We measured a frequency modulation sensitivity of  $3 \text{ GHz/V}$  and an oscillator phase noise of  $-67 \text{ dBc/Hz}$  at  $1\text{-MHz}$  offset from the carrier. The conversion loss of the single balanced rat-race hybrid mixer was  $13 \text{ dB}$  at  $94 \text{ GHz}$  with an LO power of  $6 \text{ dBm}$ . The cascode LNAs had a gain of  $8 \text{ dB}$  per stage. The output power of the transmit driver amplifier was

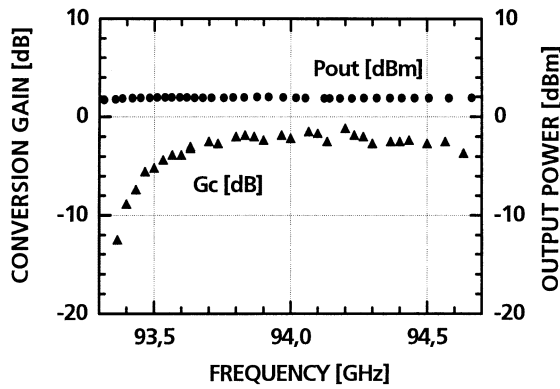


Fig. 5. Radar module #1. Measured output power and conversion gain of the receive path as a function of the frequency.

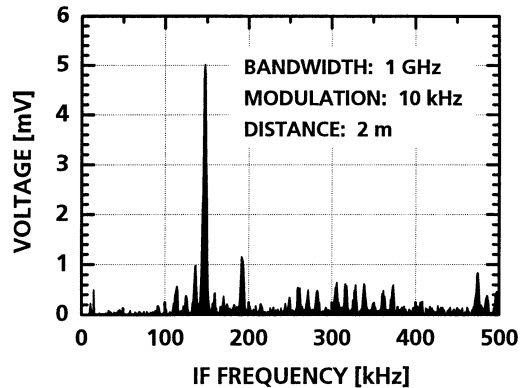


Fig. 6. IF signal of small metal target (diameter = 17 mm) at approximately 2-m distance.

10 dBm at 1-dB gain compression. The specified microstrip circulator isolation was 20 dB with an insertion loss of 1.3 dB. The waveguide-to-microstrip transition had shown an insertion loss of less than 0.5 dB, measured in a special test fixture. The bond-wire interconnections result in a reflection coefficient of approximately 10 dB due to their high characteristic impedance. We measured an output power of 2 dBm and a conversion loss of 2 dB at 50-MHz IF, as shown in Fig. 5. Due to the limited bandwidth of the circulator, as indicated by the conversion gain characteristics over frequency of the receive path shown in Fig. 5, the radar module only allows for a modulation depth of 1 GHz.

As an example of a measured radar response, the IF signal obtained from the radar reflection from a small metal coin is shown in Fig. 6. The gate bias of the oscillator was swept at a rate of 10 kHz over 0.25 V using a sawtooth waveform, resulting in a frequency-modulation bandwidth of 1 GHz and an IF frequency of 67-kHz/m distance between the antenna and target.

### III. SINGLE-CHIP 94-GHz FMCW RADAR MODULE #2 WITH INTEGRATED WILKINSON DIVIDER AND LANGE COUPLER

Due to the narrow bandwidth of the circulator, the modulation frequency of the FMCW radar module with a hexa ferrite circulator is limited. Thus, we developed a second version of the FMCW MMIC [10].

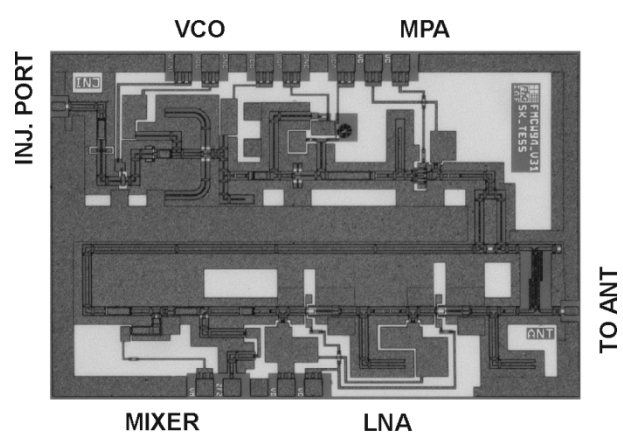


Fig. 7. Chip photograph of the 94-GHz single-chip FMCW radar MMIC #2. The chip size is 2 × 3 mm<sup>2</sup>.

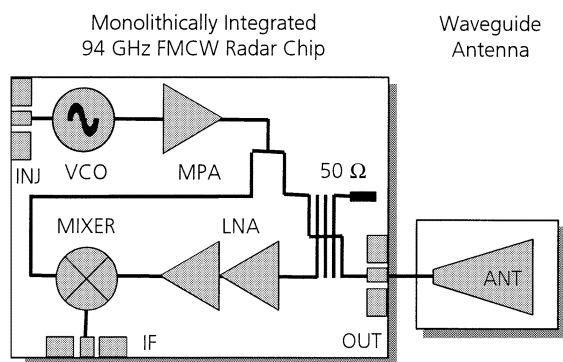


Fig. 8. Block diagram of the 94-GHz FMCW radar MMIC #2.

#### A. Circuit Design and On-Wafer Measurements

In the second design (#2), the directivity and isolation for separating the transmit and receive paths, allowing for single antenna operation, were achieved by the combination of a Wilkinson power divider and a Lange coupler. This configuration enables broad-band modulation and replaces the external circulator used in the first module, as described in Section II. The chip photograph in Fig. 7 illustrates the circuit topology of the second MMIC, using coplanar transmission lines with a metallization thickness of 3  $\mu$ m and a ground-to-ground spacing of 50  $\mu$ m. The block diagram in Fig. 8 shows the configuration of the 94-GHz FMCW radar chip. A newly developed varactor-tuned VCO offers both large tuning range and the possibility to reduce the phase noise by injection locking, as described in [11]. A very compact MPA, based on space-saving dual-gate devices, was used to amplify the oscillator signal [12]. The receive path consists of a two-stage cascode LNA and a single-ended resistive mixer. The entire chip size of the second FMCW radar MMIC is only 2 × 3 mm<sup>2</sup>.

Fig. 9 shows the on-wafer measured output power and signal frequency of the radar MMIC as a function of the tuning voltage. A tuning bandwidth of 6 GHz and an output power of approximately 2 dBm were measured by varying the varactor voltage from -3 to +1 V.

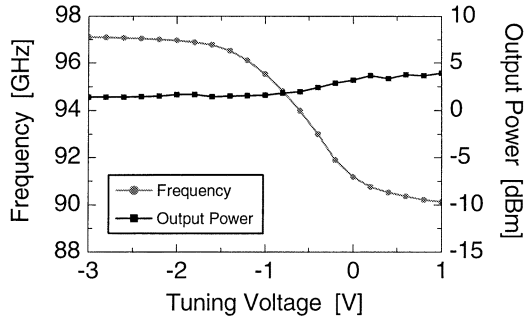


Fig. 9. 94-GHz radar MMIC #2. On-wafer measured output power and signal frequency as a function of the tuning voltage.

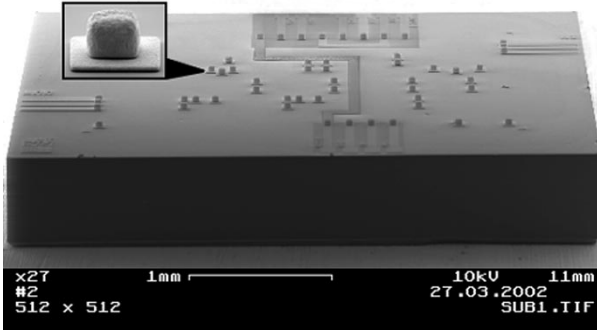


Fig. 10. Flip-chip substrate for the 94-GHz FMCW radar MMIC #2. The substrate size is  $3 \times 4 \text{ mm}^2$ .

### B. Flip-Chip Packaging on Silicon Substrates

In addition to the face-up mounting technique, we also investigated flip-chip packaging of the 94-GHz MMIC on doped n-Si substrates to further improve reproducibility and ease fabrication. Fig. 10 shows a photograph of a typical carrier substrate. The transmission lines on the substrate were realized as finite-ground coplanar waveguides (FGCPWs), to reduce the excitation of parallel-plate modes in the flip-chip substrate [13]. For good heat dissipation, the  $28\text{-}\mu\text{m}$ -high galvanic gold bumps were placed close to the active devices. Additional bumps were used to form the RF and dc contacts and to improve the mechanical stability, counteracting the different thermal expansion coefficients of GaAs and Si. In Fig. 11, the RF performance of a flip-chip-mounted radar MMIC is shown. The measured tuning bandwidth and output power correspond to the on-wafer measurement results. This shows the superior performance of the flip-chip mount due to the short low inductance interconnects.

### C. Face-Up Mounting and Module Performance

To package the coplanar 94-GHz FMCW radar MMIC in a waveguide module, a CPW-to-waveguide transition using a  $127\text{-}\mu\text{m}$ -thick quartz substrate was developed. The substrate includes the transition from the CPW of the chip to a microstrip line. At the end of the microstrip line, a small antenna patch allows a low-loss transition to the waveguide. To convert the coplanar mode into a microstrip mode, two via-holes were used, connecting the coplanar ground on the substrate surface, with the backside metallization. A photograph of a CPW-to-waveguide transition and the schematic of a bond-wire-connected pair of back-to-back transitions are shown in Fig. 12(a) and

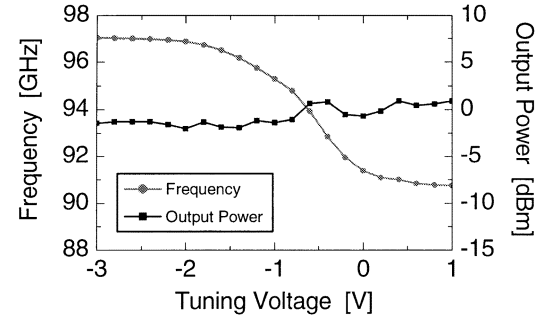


Fig. 11. Flip-chip packaged 94-GHz FMCW radar MMIC #2. Measured output power and signal frequency as a function of the tuning voltage.

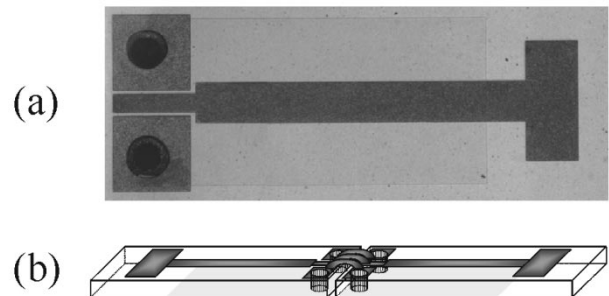


Fig. 12. (a) Photograph of a CPW-to-waveguide transition. (b) Schematic of a bond-wire-connected pair of back-to-back transitions. The wedge-bonded gold wires have a diameter of  $17\text{ }\mu\text{m}$ .

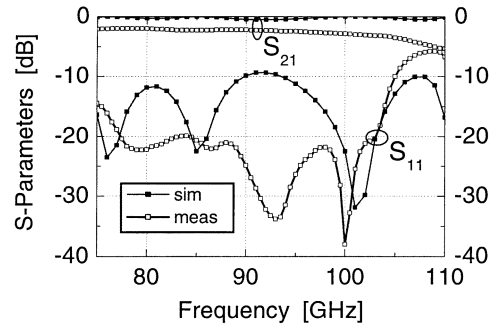


Fig. 13. Measured and simulated insertion and return losses of a pair of back-to-back transitions from 75 to 110 GHz.

(b), respectively. For the simulation and optimization of the transitions, Agilent Technology's full-wave electromagnetic (EM) High-Frequency Structure Simulator (HFSS) software was used. The  $E$ -plane probe structure was optimized to achieve a broad-band match covering the entire  $W$ -band. The simulated and measured insertion and return losses of a pair of back-to-back transitions are shown in Fig. 13. For all simulations, the metal and substrate material was assumed to be lossless. Due to this fact, and fabrication tolerances as well as via-hole,  $E$ -plane probe, and bond-wire alignment offsets, a discrepancy between the simulated and measured results is found. For the fabricated transitions, we obtained an insertion loss of approximately 2 dB from 75 to 100 GHz and a very small return loss of  $-20$  dB.

In Fig. 14, an inside view of the 94-GHz FMCW sensor module #2 is shown. For this module, the conventional face-up mounting technique was utilized. All interconnects were

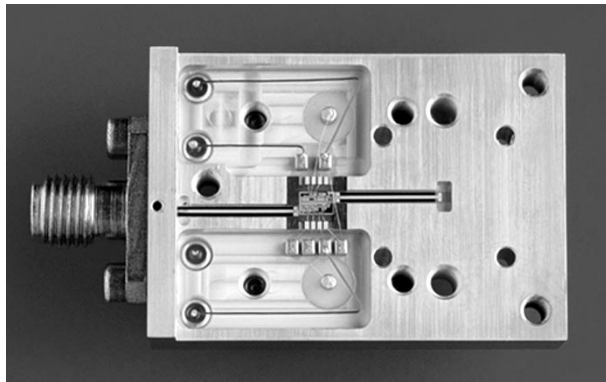


Fig. 14. Inside view of the face-up mounted 94-GHz FMCW radar module #2 with injection port.

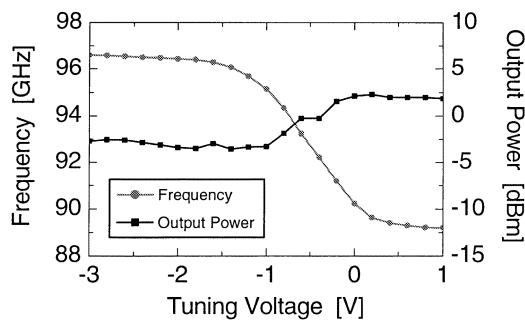


Fig. 15. 94-GHz FMCW radar module #2. Measured output power and signal frequency as a function of the tuning voltage.

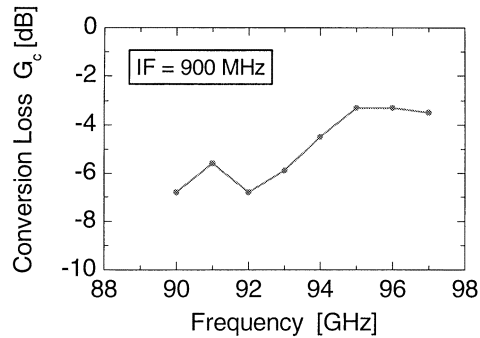


Fig. 16. Measured conversion loss of the 94-GHz FMCW radar module #2.

wedge-bonded using 17- $\mu$ m gold wires. The overall module size was 34  $\times$  24  $\times$  10 mm<sup>3</sup>. The radar sensor achieved a modulation frequency range of 6 GHz, an output power of approximately 0 dBm, and an average conversion loss of 5 dB, as shown in Figs. 15 and 16, respectively. The integration of the circulator functionality on the MMIC resulted in a significant increase of the modulation bandwidth for this module. Additionally, we could reduce the chip size and ease the fabrication process by a simple one-chip package.

#### D. Experimental Results

To verify the functionality of the FMCW sensor, it has been integrated in a measuring system comprising the sensor itself, power supply, function generator, bandpass filter, and computer

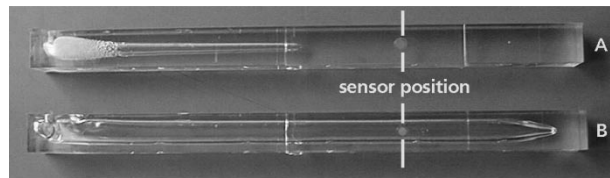


Fig. 17. Photograph of two plastic rods realized by gas-assisted injection molding.

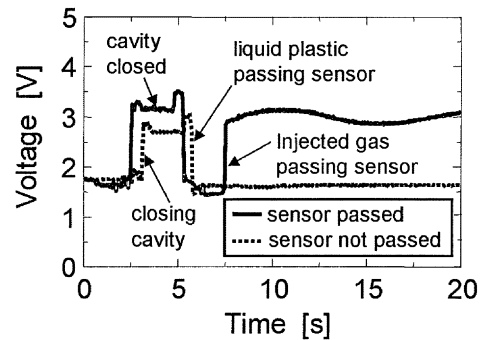


Fig. 18. IF signal of the 94-GHz FMCW radar sensor representing the time flow of the polymeric injection molding process.

with data-acquisition card. For imaging reasons, a two-axis positioning system, which allowed one- or two-dimensional scanning of the specimen, could be additionally integrated. In cooperation with the Fraunhofer Institute for Chemical Technology (ICT), Pfinztal, Germany, the module was used to monitor the quality of polymeric products in a production environment.

As an example, Fig. 17 shows two plastic rods that were manufactured by gas-assisted injection molding. During the fabrication process, liquid plastic was first filled into the mold. To reduce weight and material, gas was then injected, forming an inner cavity in the plastic rod. The radar sensor was used to monitor the gas-injection process through a Teflon window in the mold. Two experiments are represented by the two rods shown in Fig. 17. In Fig. 17(a), the gas injection stopped before the gas reached the sensor position. Fig. 17(b) shows a successful injection of the gas that has passed the sensor and, thus, led to a completely hollow plastic rod. This is illustrated furthermore in Fig. 18 by monitoring the amplitude of the IF signal during the process, clearly indicating the time flow of the injection.

Fig. 19 demonstrates that the realized measuring system is able to detect and image hidden structures like voids and defects. A 5-mm-thick and 100  $\times$  100 mm<sup>2</sup> large PVC specimen with differently deep milled letters "IZFP" was two-dimensionally scanned with the FMCW sensor. An open rectangular waveguide was used as an antenna in the near field. The distance between the antenna and specimen was approximately 2 mm. From the scanning side, the milled structures could not be seen optically. Fig. 19 shows that the milled structures can be clearly retrieved in a nondestructive and contactless way. The parallel lines around the milled letters are due to diffraction effects since the dimensions of the milled structures were in the order of magnitude of wavelength. By using focusing antennas, it will be possible to detect hidden structures over larger distances.

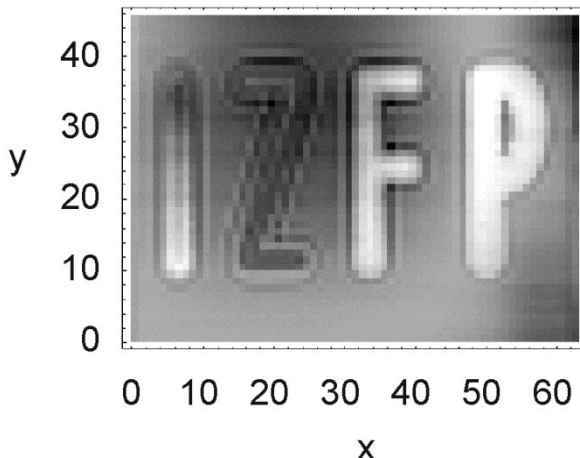


Fig. 19. Two-dimensional imaging of hidden structures in a plastic specimen in the near field.

#### IV. CONCLUSION

Two very compact single-chip  $W$ -band FMCW radar modules for high-resolution sensor applications has been demonstrated. For use with a single transmit-receive antenna, a miniature microstrip hexaferrite circulator has been integrated in the first module. This FMCW sensor achieved a tuning range of 1 GHz, an output power of 1.5 mW, and 2-dB conversion loss at 94 GHz, while occupying an chip-area of only  $7 \text{ mm}^2$ . The second module was based on a transceiver MMIC with an integrated Wilkinson divider and Lange coupler to enable both broad-band modulation and single-antenna operation. The coplanar MMIC contains four active circuits and demonstrates a tuning range of 6 GHz, a conversion loss of 5 dB, and an output power of 1 mW. The chip size could be reduced to  $6 \text{ mm}^2$ , and assembly was facilitated by a single-chip package. The FMCW radar modules were successfully used to real-time monitor the time flow of a gas-assisted injection molding process and to detect and image hidden structures in a plastic specimen. These results demonstrate the potential of compact high-resolution  $W$ -band radar sensors to improve process control, even under adverse conditions like dust, fume, heat, or vapor.

#### ACKNOWLEDGMENT

The authors would like to thank their colleagues from the Technology Department, Fraunhofer Institute for Applied Solid State Physics, Freiburg, Germany, for the fabrication of the coplanar devices, H. Massler and M. Kuri for measurements, R. Emmerich and M. Knoblauch from the Fraunhofer Institute for Chemical Technology, Pfinztal, Germany, for experimental data, and G. Weimann and M. Schlechtweg for support.

#### REFERENCES

- [1] D. C. W. Low, K. W. Chang, R. Lin, E. W. Lin, H. Wang, M. Biedenbender, G. S. Dow, and B. R. Allen, "A single-chip  $W$ -band transceiver with front-end switching receiver for FMCW radar applications," in *IEEE Microwave Millimeter-Wave Monolithic Circuits Symp. Dig.*, June 1995, pp. 225–228.
- [2] K. W. Chang, H. Wang, G. Shreve, J. G. Harrison, M. Core, A. Paxton, M. Yu, C. H. Chen, and G. S. Dow, "Forward-looking automotive radar using a  $W$ -band single-chip transceiver," *IEEE Trans. Microwave Theory Tech.*, vol. 43, pp. 1659–1668, July 1995.
- [3] M. Vossiek, T. v. Kerssenbrock, and P. Heide, "Novel nonlinear FMCW radar for precise distance and velocity measurements," in *IEEE MTT-S Int. Microwave Symp. Dig.*, June 1998, pp. 511–514.
- [4] W. H. Haydl, M. Neumann, L. Verweyen, A. Bangert, S. Kudszus, M. Schlechtweg, A. Hülsmann, A. Tessmann, W. Reinert, and T. Krems, "Single-chip coplanar 94-GHz FMCW radar sensors," *IEEE Microwave Guided Wave Lett.*, vol. 9, pp. 73–75, Feb. 1999.
- [5] T. Hirose, K. Makiyama, K. Ono, T. M. Shimura, S. Aoki, Y. Ohashi, S. Yokokawa, and Y. Watanabe, "A flip-chip MMIC design with coplanar waveguide transmission line in the  $W$ -band," *IEEE Trans. Microwave Theory Tech.*, vol. 46, pp. 2276–2282, Dec. 1998.
- [6] A. Tessmann, W. H. Haydl, T. v. Kerssenbrock, P. Heide, and S. Kudszus, "Suppression of parasitic substrate modes in flip-chip packaged coplanar  $W$ -band amplifier MMICs," in *IEEE MTT-S Int. Microwave Symp. Dig.*, May 2001, pp. 543–546.
- [7] A. Bangert, M. Schlechtweg, M. Lang, W. H. Haydl, W. Bronner, T. Fink, and B. Raynor, "W-band MMIC VCO with a large tuning range using a pseudomorphic HFET," in *IEEE MTT-S Int. Microwave Symp. Dig.*, June 1996, pp. 525–528.
- [8] A. Tessmann, W. H. Haydl, T. Krems, M. Neumann, L. Verweyen, H. Massler, and A. Hülsmann, "A compact coplanar  $W$ -band variable gain amplifier MMIC with wide control range using dual-gate HEMTs," in *IEEE MTT-S Int. Microwave Symp. Dig.*, June 1998, pp. 685–688.
- [9] Dorado Int. Corporation, "Product feature: 18 to 95 GHz microstrip ferrite devices," *Microwave J.*, pp. 158–160, Sept. 1996.
- [10] A. Tessmann, S. Kudszus, T. Feltgen, M. Riessle, C. Sklarczyk, and W. H. Haydl, "A 94 GHz single-chip FMCW radar sensor module for commercial sensor applications," in *IEEE MTT-S Int. Microwave Symp. Dig.*, vol. 3, June 2002, pp. 1851–1854.
- [11] S. Kudszus, T. Berceli, A. Tessmann, M. Neumann, and W. H. Haydl, "W-band HEMT-oscillator MMIC's using subharmonic injection locking," in *IEEE Trans. Microwave Theory Tech.*, vol. 48, Dec. 2000, pp. 2526–2532.
- [12] A. Tessmann, W. H. Haydl, M. Neumann, S. Kudszus, and A. Hülsmann, "A coplanar  $W$ -band power amplifier MMIC using dual-gate HEMTs," in *Proc. 29th Eur. Microwave Conf.*, vol. 1, Oct. 1999, pp. 246–249.
- [13] M. Yu *et al.*, "W-band InP HEMT MMIC's using finite-ground coplanar waveguide (FGCPW) design," *IEEE J. Solid-State Circuits*, vol. 34, pp. 1212–1217, Sept. 1999.



**Axel Tessmann** was born in Freiburg, Germany, in 1969. He received the Dipl.-Ing. degree in electrical engineering from the Technische Hochschule Karlsruhe, Karlsruhe, Germany, in 1997.

He then joined the High Frequency Devices and Circuits Department, Fraunhofer Institute for Applied Solid State Physics (IAF), Freiburg, Germany, where he is involved in the modeling of active and passive components and the design and packaging of MMICs and subsystems up to  $D$ -band frequencies.



**Steffen Kudszus** (S'99–A'01–M'02) received the Diplom-Ingenieur degree in electrical engineering from the University of Stuttgart, Stuttgart, Germany in 1996, and the Dr-Ingenieur (Ph.D.) degree from the University of Karlsruhe, Karlsruhe, Germany, in 2001.

In 1996, he joined the High Frequency Devices and Circuits Department, Fraunhofer Institute for Applied Solid State Physics (IAF), Freiburg, Germany. Since 2001, he has been with Big Bear Networks, Milpitas, CA, where he is involved with the development of integrated circuits for high-speed communication at 40 Gb/s. His main research areas were the design of MMICs using HEMTs on GaAs and InP, simulation, and linear and nonlinear device modeling up to 140 GHz. He concentrated his research on microwave and millimeter-wave oscillators with novel stabilization techniques, covering all aspects of simulation, design, and high frequency,  $1/f$ -noise, and phase-noise measurements.



**Tobias Feltgen** was born in Emmendingen, Germany, in 1970. He received the Diploma degree in mineralogy from the University of Freiburg, Freiburg, Germany, in 1997, and the Ph.D. degree from the University of Freiburg, Freiburg, Germany, in 2001.

From 1997 to 2001, he was with the Material Research Center Freiburg (FMF), where he was involved with crystal growth and process technology of II–VI materials. He is currently with the Process Technology Department, Fraunhofer Institute for Applied Solid State Physics (IAF), Freiburg, Germany, where he is involved with the process technology of GaAs- and GaN-based HEMTs.



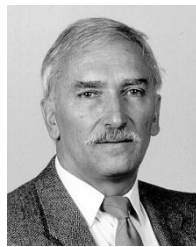
**Christoph Sklarczyk** was born in Zabrze, Poland, on January 24, 1953. He received the Doctor of Natural Sciences degree from the University of Saarland, Saarbrücken, Germany, in 1982.

Since 1982, he has been a Physicist with the Fraunhofer Institute for Nondestructive Testing (IZFP), Saarbrücken, Germany. His research and development interests comprise nondestructive testing by microwaves, ultrasound, and acoustic emission including signal processing and imaging.



**Markus Riessle** was born in Freiburg, Germany, in 1962. He received the Certified Engineer degree in mechanical engineering from the Gewerbeschule Freiburg, Freiburg, Germany, in 1994.

From 1995 to 1999, he was with Raymond, Weil, Germany, where he was engaged in the design and layout of injection molding components for the automotive industry. In 2000, he joined the High Frequency Devices and Circuits Department, Fraunhofer Institute for Applied Solid State Physics (IAF), Freiburg, Germany, where he is currently involved in the packaging of millimeter-wave subsystems and modules up to 100 GHz.



**William H. Haydl** was born in 1939. He received the B.Sc. degree in electrical engineering from the Illinois Institute of Technology, Chicago, in 1962, and the M.Sc. and Ph.D. degrees from Stanford University, Stanford, CA, in 1964 and 1967, respectively.

He was then with the Fairchild Semiconductor Research Laboratory and the Rockwell Science Center Research Laboratory. Since 1970, he has been with the Fraunhofer Institute for Solid State Physics (IAF), Freiburg, Germany. His areas of research have included III–V material technology, including molecular beam epitaxy, surface acoustic-wave devices, charge-coupled devices (CCDs), and microwave and millimeter-wave devices, such as Gunn, IMPATT, and mixer diodes. While with the IAF, he has concentrated his effort on microwave and millimeter-wave heterojunction field-effect transistors and integrated circuits, advancing the art of coplanar MMICs and associated packaging techniques. From 1990 to 1992, he performed research on InP-based HEMTs at Cornell University.

Dr. Haydl is a member of Tau Beta Pi, Sigma Pi and Eta Kappa Nu. He was the recipient of the 1985 and 1993 Fraunhofer Prize.